Proceedings of the VIII International Conference ION 2010, Kazimierz Dolny, Poland, June 14–17, 2010

Nanocrystal- and Dislocation-Related Luminescence in Si Matrix with InAs Nanocrystals

F. Komarov[a,*], L. Vlasukova[a], O. Milchanin[a], A. Mudryi[b], J. Zuk[c], K. Pyszniak[c] and M. Kulik[c]

[a]Belarussian State University, Nezavisimosti ave. 4, 220030 Minsk, Belarus

[b]Scientific and Practical Materials Research Center, National Academy of Sciences of Belarus P. Brovki Str. 17, 220072 Minsk, Belarus

[c]Institute of Physics, Maria Curie-Skłodowska University, pl. M. Curie-Skłodowskiej 1, 20-031 Lublin, Poland

We have studied the influence of ion implantation and post-implantation annealing regimes on the structural and optical properties of silicon matrix with ion-beam synthesized InAs nanocrystals. (100) Si wafers were implanted at 25 and 500 °C, subsequently with high fluences of As and In ions. After implantation the samples were processed by furnace and rapid thermal annealing at 900, 950 and 1050 °C. A part of the samples implanted at 25 °C was additionally exposed to H_2^+ ions (100 keV, 1.2×10^{16} cm^{-2} in terms of atomic hydrogen). This procedure was performed to obtain an internal getter. In order to characterize the implanted samples transmission electron microscopy and low-temperature photoluminescence techniques were employed. It was demonstrated that by introducing getter, varying the ion implantation temperature, ion fluences and post-implantation annealing duration, and temperature it is possible to form InAs nanocrystals in the range of sizes of 2–80 nm and create various concentration and distribution of different types of secondary defects. The last ones cause in turn the appearance in photoluminescence spectra dislocation-related D1, D2 and D4 lines at 0.807, 0.870 and 0.997 eV, respectively.

PACS: 78.66.−w, 78.60.Fi

1. Introduction

A silicon based optoelectronics progress is restrained because of the absence of effective light source — light emitting diode or laser. The main problem is the indirect band gap nature of silicon, resulting in inefficient light emission. A number of approaches to overcome this problem were reported including the synthesis of A^3B^5 quantum dots [1], or the controlled formation of structural defects in Si matrix [2, 3]. In this work, we present the results of structural and optical characterizations of Si layers with ion-beam synthesized InAs nanocrystals.

2. Experimental

(100) Si wafers were implanted at 25 and 500 °C subsequently with As and In ions. We have performed two types of experiment differing in ion implantation and post-implantation annealing regimes. In the first type of experiment Si samples were implanted with As (245 keV, 4.1×10^{16} cm^{-2}) and In ions (350 keV, 3.7×10^{16} cm^{-2}). Afterwards, the samples were annealed at 900 °C for 60 min. In the second type of experiment ion energies and fluences were reduced by a factor of 1.5. Accordingly, in this case silicon samples were implanted with As (170 keV, 3.2×10^{16} cm^{-2}) and In (250 keV, 2.8×10^{16} cm^{-2}). After that, the implanted samples were annealed at 950 and 1050 °C for 3 min using rapid thermal annealing (RTA). In the both experiments a part of the samples implanted at the room temperature was additionally exposed to H_2^+ ions (100 keV, 1.2×10^{16} cm^{-2} in terms of atomic hydrogen). This procedure was performed to obtain an internal getter at a depth of about 500 nm during post-implantation annealing. In both cases the annealing was carried out in an inert ambient gas.

A structure of the implanted samples was studied by means of transmission electron microscopy (TEM) in both plane-view (PV) and cross-section (X) geometry. The TEM investigations were performed using a Hitachi H-800 instrument operating at 200 keV. The samples prepared for the TEM measurements have to be transparent for probe electron beam. It is possible if their thickness does not exceed 150–200 nm. For this reason for detailed investigations of deeper regions into crystal bulk we combined PV-TEM preparation with the precise removal of thin layers from the face surface of sample.

* corresponding author; e-mail: KomarovF@bsu.by

The optical properties of samples were investigated by means of low temperature photoluminescence (PL). PL spectra were taken in the spectral region of 0.7 to 2 eV. The samples were mounted in a liquid He immersion cryostat. The 514.5 nm line of an argon ion laser was used to induce PL. The luminescence was dispersed by a 0.6 m grating monochromator and detected by a cooled InGaAs detector.

3. Results and discussion

TEM and PL results for the samples implanted with the higher ion fluence are presented in Fig. 1. For the sample implanted with As and In at room temperature with an additional implantation of H_2^+, a thin layer of secondary defects (mostly dislocation loops) is recorded at a depth of approximately 500 nm, around the R_p for H_2^+ ions (Fig. 1a). The formation of such defects is characteristic process of amorphous layer recrystallization.

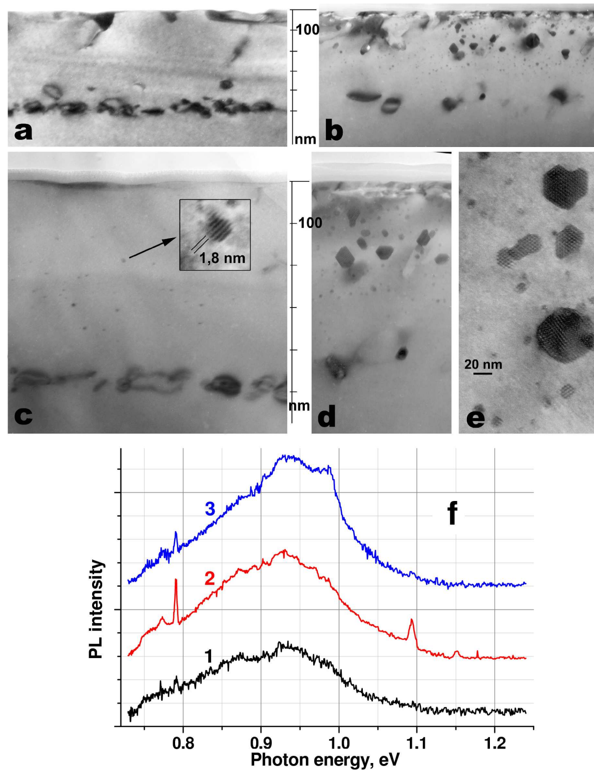

Fig. 1. TEM cross-section (a–d) and plan-view (e) images as well as PL spectra (f) of the silicon samples implanted with As (245 keV, 4.1×10^{16} cm^{-2}) and In (350 keV, 3.7×10^{16} cm^{-2}) and annealed at 900 °C for 60 min. $t_{\mathrm{impl}} = 25$ (a, c, curves 1 and 2 in f) and 500 °C (b, d, e, curve 3 in f). The samples with getter layer — a, c, curve 2 in f. Inset in (c) represents an image of InAs precipitate taken at higher magnification.

At depths from 100 to 350 nm, there are small precipitates from 2 to 10 nm in size. This region in the crystal corresponds to concentration maxima in the implanted impurity profiles simulated using SRIM-2003 code. A detailed study of the structure of these inclusions, according to the technique described in [1], allowed us to identify them as InAs nanocrystals. One can see from Fig. 1b that in the case of "hot" implantation two spatially separated layers of secondary defects are observed. The first defect layer containing micropores and microtwins is localized in the thin near surface region. In the deeper defect layer (400–450 nm), separate dislocation loops are recorded. Between these two defect layers, at the sample depth of 80–350 nm, there is a defect-free silicon region containing InAs precipitates. Alongside the small clusters (from 2 nm), considerably larger ones with sizes up to 80 nm are observed (Fig. 1b). Figure 1f depicts the PL spectra of implanted and annealed samples. For the crystals implanted at 25 °C, a broad band in a range of 0.75–1.1 eV with a maximum of 0.93 eV is detected in PL spectra. The intensity of this band is almost five times greater for the sample with a getter layer in comparison with one without getter (curves 2 and 1 in Fig. 1f, respectively). A phononless line of 0.79 eV is observed in the spectrum, due to the recombination of bound excitons on ion induced defects (interstitial carbon–interstitial oxygen (C_i–O_i pairs) [3]. For the samples implanted at 500 °C, a broad band in the range 0.75–1.1 eV with an extended low energy wing is also found in the PL spectra (curve 3 in Fig. 1f). The intensity of this band is four times greater than that of samples implanted at room temperature (Fig. 1f, curve 1).

Figure 2 shows TEM plan-view images and PL spectra of samples implanted with the lower fluence after RTA at 1050 °C for 3 min. On the plan-view images of the subsurface region up to depth of about 150–200 nm one can see nanocrystals. The size of nanocrystals varies in the range of about 5–40 nm as in the both samples with and without getter layer (Fig. 2a, c). On the depth of about 200–400 nm a layer of secondary defects is located (Fig. 2b, d). The existence of getter layer influences sizes and density of secondary defects. One can see that in the sample without getter layer there are large elongated and curved dislocation-like defects. There also should be noted disordered zones marked by arrows in Fig. 2d. The size of the largest disordered zones tends to ≈ 500 nm. The getter layer creation results in a large number of small densely packed dislocation loops (Fig. 2b). As one can see from Fig. 2e, an intense band at 1.09 eV corresponding to the Si band-edge emission dominates the PL spectra. A broad band in a region 0.85–1.05 eV is also detected. We may assume that this band is a superposition of at least two PL lines with maxima of about 0.960 and 0.995 eV. In the PL spectrum of the sample with getter an additional weak line with a maximum of 0.807 eV is detected. The emission at 0.995 eV and at 0.807 eV coincides to the energies of so-called D1 and D4 lines and may be attributed to the presence of dislocations in implanted layers. The dislocation-related PL peaks with maxima at 0.807 eV (D1) and at 0.870 eV (D2) were detected in plastically deformed Si [4], Er-

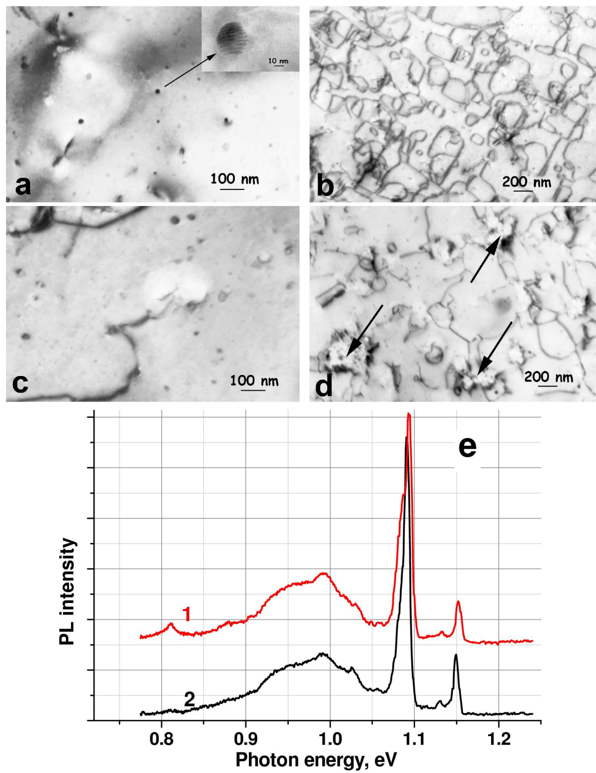

Fig. 2. TEM plan-view images (a–d) and PL spectra (e) of the samples implanted with As (170 keV, 3.2×10^{16} cm^{-2}) and In (250 keV, 2.8×10^{16} cm^{-2}) at 25 °C and annealed at 1050 °C for 3 min. The samples with getter layer (a, b, curve 1 in e) and without getter layer (c, d, curve 2 in e). Inset in (a) represents a precipitates image taken at higher magnification.

-implanted silicon [3], relaxed epitaxial SiGe layers [5], laser-melted Si [6] and liquid-phase epitaxy Si [7]. The dislocation-related peaks at 0.935 (D3) and at 0.997 eV (D4) were found in Si wafers after the formation of oxygen precipitates [8]. Photoluminescence at 0.960 eV was detected for coherent InAs clusters on Si (001) fabricated by means of MBE-technique [9] and by means of high fluence implantation of As and In ions [1]. The appearance of PL signal at 0.960 eV was attributed to the formation of InAs quantum dots in the silicon matrix.

TEM plan-view images and PL spectra for samples implanted with As (170 keV, 3.2×10^{16} cm^{-2}) and In (250 keV, 2.8×10^{16} cm^{-2}) at 500 °C and annealed at 950 or 1050 °C for 3 min are presented in Fig. 3. It is worth to note that for "hot" implantation conditions nanocrystal size increases significantly in comparison with the implantation at 25 °C (Fig. 3a, b; Fig. 2a, c). The largest precipitates have a size of about 100 nm. The density of precipitates in "hot" implanted samples is also higher in comparison with the samples implanted at the room temperature.

In TEM patterns (insets in Fig. 3a, c) there are distinct reflexes from microtwins. It should be noted that in the dark-field image precipitates sizes seem to be larger in comparison with bright-field image (Fig. 3a, b). This effect is caused of "glowing" of nanocrystal/Si matrix interfaces. One can see a great number of small (2–5 nm) clusters in the dark-field image (Fig. 3b).

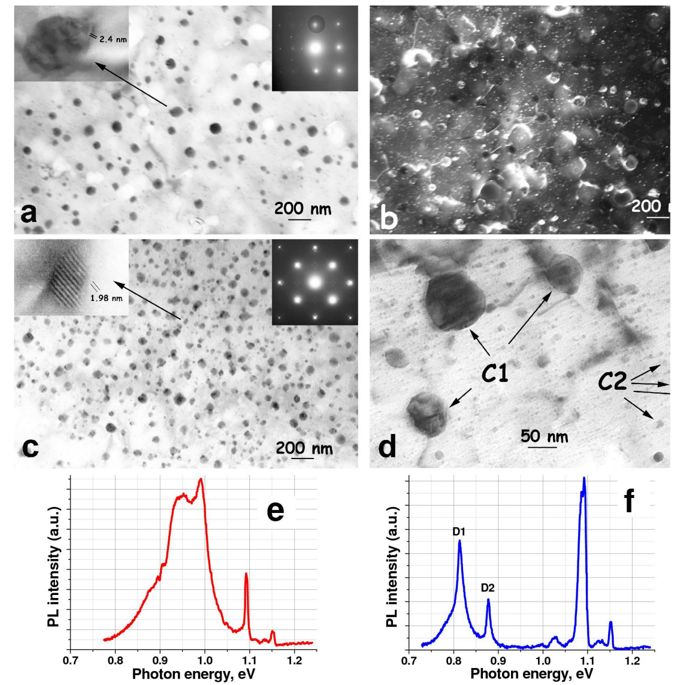

Fig. 3. TEM bright-field (a, c, d) and dark-field (b) plan-view images and PL spectra (e, f) of the samples implanted with As (170 keV, 3.2×10^{16} cm^{-2}) and In (250 keV, 2.8×10^{16} cm^{-2}) at 500 °C and annealed at 1050 (a, b, e) and 950 °C (c, d, f) for 3 min. Left-side insets in (a, c) are precipitates images taken at higher magnification.

Figure 3d demonstrates a bimodal size distribution of nanocrystals in the samples annealed at 950 °C.

Figure 3e shows the PL spectrum of the sample annealed at 1050 °C. As for the room temperature implanted sample, two lines are found in the spectrum. They are a narrow line at 1.09 eV corresponding to the Si band-edge emission and a very intensive broad band in a region of 0.85–1.05 eV with an extended low-energy wing. Unlike the room temperature implanted sample, in the sample after "hot" implantation the 1.09 eV peak's intensity is lower in comparison with the band in the range of 0.85–1.05 eV.

Figure 3f shows the PL spectrum of the sample annealed at 950 °C for 3 min. Surprisingly, the reduction of the annealing temperature results in the rearrangement of photoluminescence signal and an appearance of intensive dislocation-related D1 and D2 bands at 0.807 eV and 0.870 eV. An intensity of the Si band-edge emission related peak at 1.09 eV increases while a broad band in a region of 0.85–1.05 eV is not detected. It should be noted that in accordance with the TEM data there is no

significant difference in the region with maximum density of nanocrystals for the samples annealed at 950 and 1050 ℃.

Further investigations to study the mechanism of structural-phase transformations in InAs nanocrystals/Si matrix system after RTA and to clear the nature of secondary defects resulting in the appearance of dislocation-related lines in PL spectra are in progress.

4. Conclusions

The influence of ion implantation and post-implantation annealing regimes on the structural and optical properties of silicon matrix with ion-beam synthesized InAs nanocrystals has been studied. It was demonstrated that the introduction of the getter layer and varying the post-implantation annealing duration and temperature may provide the way for controlled generation of secondary defects and the appearance in PL spectra of dislocation-related D1, D2 and D4 bands at 0.807, 0.870, and 0.997 eV, respectively.

Acknowledgments

This work was supported by the Belarussian Republican Foundation for Fundamental Research (grants F10R-143 and T10R-142).

References

[1] F. Komarov, L. Vlasukova, W. Wesch, A. Kamarou, O. Milchanin, S. Grechnyi, A. Mudryi, A. Ivaniukovich, *Nucl. Instrum. Methods Phys. Res. B* **266**, 3557 (2008).

[2] M.A. Lorenço, M. Milosavljević, R.M. Gwilliam, K.P. Homewood, G. Shao, *Appl. Phys. Lett.* **87**, 201105 (2005).

[3] N.A. Sobolev, O.B. Gusev, E.I. Shek, V.I. Vdovin, T.G. Yugova, A.M. Emel'yanov, *J. Lumin.* **80**, 357 (1999).

[4] V.V. Kveder, E.A. Steinmann, S.A. Shevchenko, H.G. Grimmeiss, *Phys. Rev. B* **51**, 10520 (1995).

[5] S. Fukatsu, Y. Mera, M. Inoue, K. Maeda, H. Akiyma, H. Sakaki, *Appl. Phys. Lett.* **68**, 1889 (1996).

[6] E.Ő. Sveinbjőrnsson, J. Weber, *Mater. Res. Soc. Symp. Proc.* **422**, 148 (1996).

[7] S. Binetti, M. Donghi, S. Pizzini, A. Kataldini, *State Phenomena* **57-58**, 197 (1997).

[8] R. Sauer, J. Weber, J. Sholz, E.R. Weber, K.H. Kusters, H. Alexander, *Appl. Phys. A* **36**, 1 (1985).

[9] R. Heitz, N.M. Ledentsov, D. Bimberg, R. Heitz, N.N. Ledentsov, D. Bimberg, A.Yu. Egorov, M.V. Maximov, V.M. Ustinov, A.E. Zhukov, Zh.I. Alferov, G.E. Cirlin, I.P. Soshnikov, N.D. Zakharov, P. Werner, U. Gösele, *Physica E* **7**, 317 (2000).